

## MICROSTRUCTURE OF YTTRIA-STABILIZED ZIRCONIA NANOMATERIALS STUDIED BY POSITRON ANNIHILATION SPECTROSCOPY

Ivan PROCHÁZKA<sup>a</sup>, Jakub ČÍŽEK<sup>a</sup>, Oksana MELIKHOVA<sup>a</sup>, Jan KURIPLACH<sup>a</sup>,  
Tetyana E. KONSTANTINOVA<sup>b</sup>, Igor A. DANILENKO<sup>b</sup>

<sup>a</sup> Charles University in Prague, Faculty of Mathematics and Physics, Department of Low Temperature Physics, V Holešovičkách 2, CZ-180 Prague 8, Czech Republic, [ivan.prochazka@mff.cuni.cz](mailto:ivan.prochazka@mff.cuni.cz)

<sup>b</sup> Galkin Donetsk Institute for Physics and Engineering, National Academy of Science of Ukraine, Luxemburg Street 72, 83114 Donetsk, Ukraine

### Abstract

Investigations of several yttria-stabilized zirconia (YSZ) pressure-compacted nanopowders are reported. Positron annihilation spectroscopy is employed as the main experimental tool. The defects associated with grain boundaries (GB's), the mean grain size and its growth during sintering nanopowders, the nanoporosity, an influence of the material composition on the final microstructure and a possible segregation of different kinds of atoms at GB's are discussed. The main attention will be focused on the role of chromia addition to YSZ. Positrons are trapped predominantly (i) in the monovacancy-like defects situated along GB's or (ii) at the triple junctions of GB's. PAS is then used for estimation of grain size. A small amount of chromia additive is shown to lead to a lower mean grain size of the initial YSZ nanopowders.

### 1. INTRODUCTION

Zirconium dioxide ( $ZrO_2$ , zirconia) exhibits a high melting point of 2700 °C, low electronic as well as thermal conductivities and good oxygen-ion conductivity at higher temperatures. Zirconia possesses, moreover, favourable mechanical properties (enhanced strength and fracture toughness) [1]. These features predestine zirconia for a variety of applications, e.g., as refractory ceramics, ceramic glazes, thermal-barrier coatings, electroceramics, insulators, solid oxide fuel cells, oxygen sensors as well as abrasives, grinding media and machining tools. The advantageous characteristics of  $ZrO_2$ -based materials become improved when these materials are manufactured of nanoscopic powders.

Applications of the *pure* zirconia at elevated temperatures are strongly limited due to the phase transition from the room-temperature monoclinic (*m*) to the denser tetragonal (*t*) phase at  $\approx 1200$  °C [1]. Large volume changes take place during this transition, creating cracks within the lattice structure. The pure zirconia becomes cubic (*c*) at temperatures raised above  $\approx 1380$  °C. The high temperature zirconia phases are stabilized at room temperature if a small amount of the trivalent yttrium oxide ( $Y_2O_3$ , yttria) is introduced as a solid solution in the  $ZrO_2$  lattice [1]. Such a system is referred to as the yttria-stabilized zirconia (YSZ). It remains cubic in a wide temperature range when more than  $\approx 8$  mol. % of the yttria stabilizer is added (fully stabilized YSZ). If the yttria admixture amounts  $\approx 3$  mol. %, YSZ structure becomes tetragonal after heating above 1000 °C and the *t*-phase is metastable below 1000 °C where it coexists with the monoclinic one (partially stabilized YSZ).

Because of stoichiometry violation, an addition of the  $Y_2O_3$  stabilizer introduces a large amount of native O vacancies or their aggregates with a metal atom in the  $ZrO_2$  host lattice. Further types of open-volume defects become of importance in the YSZ *nanomaterials* due to a significant volume fraction occupied by grain boundaries (GB's): GB-associated vacancy-like misfit defects, vacancy clusters at GB's intersections (triple points), voids and pores. It may be expected that such defect structures influence the macroscopic properties of YSZ nanomaterials. Currently, there is also a growing interest in  $ZrO_2$ -based materials

containing beside the Y also the Cr atoms dissolved in the zirconia lattice. Obviously, more complex defect configurations involving new kinds of defects are to be expected in such a *ternary* solid oxide solution compared to the  $ZrO_2$  containing only the yttria stabilizer (below, the latter kind of systems is referred to as the *binary* YSZ).

From the point of designing YSZ materials according to specific industrial demands, the nature and behaviour of nanometer-sized open-volume defects are significant factors. Positrons are known to probe these kinds of defects with a high sensitivity. Thus positron annihilation spectroscopy (PAS) represents an efficient tool of investigations on nanomaterials. In the present Contribution, our recent results [2] of PAS characterisation of defects in the *m*-, *t*- and *c*-YSZ pressure-compacted nanopowders and sintered ceramics will be briefly reviewed. Then, new data on an effect of the chromia addition to the *t*-YSZ nanopowders will be reported. At the preceding NANOCON Conference, a potential of PAS techniques for studies of ultra fine-grained metals has been illustrated [3,4]. The present Contribution is also an extension of these attempts giving an illustration of PAS applicability to investigations of the oxide nanomaterials.

## 2. OVERVIEW OF PAS

When an energetic positron (with kinetic energy well above that of thermal motion) is implanted into a material to be studied, it will quickly lose its energy until reaching thermal equilibrium with surroundings. Then the positron makes thermal diffusion movement through the medium. During thermal-diffusion stage, positrons may become trapped in open-volume defects (various vacancy-like structures, dislocations, vacancy clusters). In insulators or in materials containing nanometer-sized pores, moreover, positron may pick up an electron of the medium to form positronium (Ps) – a bound state of an electron-positron pair. The para- or ortho-Ps (pPs or oPs, respectively) are created with formation probabilities constituting a ratio of 1:3. Finally, the positron annihilates a surrounding electron. The annihilation event is accompanied by emission of two energetic photons which convey information about the electronic structure at the annihilation site and about the positron state at the moment of annihilation. The photons escape outside the sample to photon detectors what makes PAS to be a non-destructive technique of materials research.

The two basic PAS observables are the positron lifetime (PLT) and the electron momentum. The latter quantity is measured as the Doppler shift in energy of annihilation photons. The PLT is primarily the positron response to a local electron density at the annihilation site. Thus the measurements of PLT allow for judgement of the type of defects capable to trap positrons, i.e., the size of open volume associated to such a defect. Moreover, information about defect concentrations can also be deduced. Typical PLT values amount  $0.15 \div 0.35$  ns for vacancy-like defects in semiconductors and insulators, detection threshold for monovacancies may appear to be as low as  $10^{16} \text{ cm}^{-3}$ . Doppler broadening (typically  $\approx 1$  keV) due to electron momentum distribution provides additional information about the role of positron trapping. The coincidence Doppler broadening experiments (CDB) disclose the contribution of the inner electronic shells and provide thus unrivalled data on chemical surrounding of the annihilation site (defect). For example, the defect – impurity atom complexes may be identified in this way.

Positron diffusion is characterized by diffusion lengths falling typically in a range of 50 to 200 nm in media with low defects concentrations. Hence in materials with grain size below  $\approx 300$  nm, positrons may easily diffuse toward GB's, get trapped at defects there and thus probe also their structure.

Porosity which may rise in nanopowders and nanoceramics can be investigated via observations of oPs decays by a two-photon pick-off process characterized with lifetimes above 1 ns. The pore size can be estimated from the observed oPs pick-off lifetimes using appropriate semiempirical models, see Ref. [5].

### 3. EXPERIMENTS

**Samples.** The initial YSZ nanopowders studied in the present work were made from stoichiometric compositions of water solutions of  $ZrO_2(NO_3)_2$ ,  $Y(NO_3)_3$  and  $CrCl_3 \cdot 6H_2O$  using a co-precipitation process. The detailed description of this procedure can be found elsewhere [6,7]. The nanopowders were calcinated in air at  $600 \div 700$  °C for 2 h (binary YSZ) or 1 h (ternary YSZ) and then compacted under an uniaxial pressure of 500 MPa into tablets of  $\approx 10$  mm diameter and  $\approx 5$  mm thickness. The binary YSZ powders were pressure-compacted also under 250 and 500 MPa in order to examine possible pressure effects. The chemical purity of the initial nanopowders was checked by X-ray fluorescence analysis and the results were given in the preceding paper [2]. The phase content and the mean grain size of the nanopowders were determined by X-ray diffraction (XRD). The composition of the compacted binary and ternary YSZ nanopowders studied in this work and the mean grain size from XRD are listed in table 1.

Sintering process was investigated on the binary *t*-YSZ sample compacted under 500 MPa. The samples were sintered for 2 h in air at three different temperatures  $T_S$ : 1000, 1200 and 1350 °C.

**Table 1**

The basic characteristics of the binary and ternary YSZ nanopowders studied in the present work.

| Sample                                  |         | Phase    | Mean grain size [nm] |
|---|---------|----------|----------------------|
| composition                             | abbrev. |          |                      |
| pure $ZrO_2$                            | Z0Y     | <i>m</i> | 23.2                 |
| $ZrO_2+3mol.\% Y_2O_3$                  | Z3Y     | <i>t</i> | 17.6                 |
| $ZrO_2+8mol.\% Y_2O_3$                  | Z8Y     | <i>c</i> | 15.6                 |
| $ZrO_2+3mol.\% Y_2O_3+0.3mol.\%Cr_2O_3$ | Z3Y0.3C | <i>t</i> |                      |
| $ZrO_2+3mol.\% Y_2O_3+0.7mol.\%Cr_2O_3$ | Z3Y0.7C | <i>t</i> |                      |
| $ZrO_2+3mol.\% Y_2O_3+1.5mol.\%Cr_2O_3$ | Z3Y1.5C | <i>t</i> |                      |
| $ZrO_2+3mol.\% Y_2O_3+2.9mol.\%Cr_2O_3$ | Z3Y2.9C | <i>t</i> |                      |
| $ZrO_2+3mol.\% Y_2O_3+5.0mol.\%Cr_2O_3$ | Z3Y5.0C | <i>t</i> |                      |

In addition, the well-annealed pure Fe, Zr, Y and Cr metal samples were used as the reference ones in PLT or CDB measurements. These specimens could be regarded as defect-free materials in which virtually all positrons are annihilated from the delocalized state [2].

**Apparatus and data taking.** The positron source ( $\approx 1.3$  MBq of the iThemba LABS carrier-free  $^{22}Na_2CO_3$  salt sealed between two

4  $\mu$ m thick Dupont mylarC foils) was sandwiched between two identical tablets of the material studied. The sandwich was then put at the working position of the PLT or CDB spectrometer.

The fast-fast modification of a  $BaF_2$  spectrometer [8] was used for the PLT measurements. The spectrometer exhibited a time resolution of  $160 \div 170$  ps (FWHM for  $^{22}Na$ ) and a peak-to-background ratio better than  $10^3$ . At least  $10^7$  coincidence events were recorded in each PLT spectrum. Decompositions of measured PLT spectra into individual components was performed using the maximum-likelihood method.

A two-detector (HPGe-HPGe) spectrometer [9] was employed in the CDB measurements. The spectrometer exhibited an energy resolution of 1.1 keV (FWHM at 511 keV  $\gamma$ -ray energy) and a peak-to background ratio of  $\approx 10^5$ . At least  $10^8$  coincidence events were accumulated in each two-dimensional CDB spectrum. The CDB results are represented below as the ratios of the Doppler-broadened profiles (DBP's) shown by the samples studied to the DBP of the pure Zr reference specimen.

#### 4. RESULTS & DISCUSSION

**Binary YSZ's.** The results of the PLT measurements on the pressure compacted binary and ternary YSZ nanopowders were summarized in table 2. The four-component PLT spectra were exhibited by the binary YSZ nanopowders and were treated in details in our preceding paper [2]. Since no pronounced dependence of PLT data on compacting pressure was observed [2] we confine in table 2 to the data obtained for 500 MPa. Below, we review main results of that study: (i) The shortest positron lifetime,  $\tau_1 \approx 0.185$  ns, obviously originates from positron trapping in monovacancy-like defects. (ii) The medium lifetime,  $\tau_2 \approx 0.375$  ns, results from positron trapping by larger defects of open volume comparable to a few-vacancy aggregates. (iii) The two longest lifetimes,  $\tau_3 \approx 2.0$  ns and  $\tau_4 \approx 30$  ns, testify that the Ps formation and subsequent oPs annihilation. in voids and nanopores, respectively, occur in the sample.

**Table 2**

Positron lifetimes  $\tau_i$  and relative intensities  $I_i$  observed in compacted YSZ nanopowders. Data for the binary systems are taken from ref. [2]. Normalization of  $I_1+I_2+4(I_3+I_4)/3=100\%$  is used and the pPs contribution is not shown. The standard deviation errors are given in parentheses in the units of the last significant digit.

| Sample  | $\tau_1$ [ns] | $I_1$ [%] | $\tau_2$ [ns] | $I_2$ [%] | $\tau_3$ [ns] | $I_3$ [%] | $\tau_4$ [ns] | $I_4$ [%] |
|---------|---------------|-----------|---------------|-----------|---------------|-----------|---------------|-----------|
| Z0Y     | 0.187 (3)     | 42 (2)    | 0.377 (4)     | 48 (2)    | 1.8 (1)       | 1.5 (1)   | 31 (2)        | 5.7 (3)   |
| Z3Y     | 0.174 (3)     | 27 (2)    | 0.373 (3)     | 63 (2)    | 1.6 (1)       | 1.4 (1)   | 30 (2)        | 5.9 (3)   |
| Z8Y     | 0.185 (3)     | 30 (2)    | 0.365 (4)     | 60 (2)    | 2.2 (1)       | 2.1 (1)   | 26 (2)        | 5.0 (3)   |
| Z3Y0.3C | 0.191 (3)     | 31.4 (9)  | 0.381 (2)     | 68.6 (9)  |               |           |               |           |
| Z3Y0.7C | 0.191 (3)     | 26.0 (8)  | 0.390 (2)     | 74.0 (8)  |               |           |               |           |
| Z3Y1.5C | 0.190 (4)     | 20.6 (8)  | 0.387 (2)     | 79.4 (8)  |               |           |               |           |
| Z3Y2.9C | 0.209 (2)     | 20.0 (10) | 0.398 (5)     | 80.0 (10) |               |           |               |           |
| Z3Y5.0C | 0.259 (14)    | 20.0 (20) | 0.393 (4)     | 80.0 (20) |               |           |               |           |

Note that no components belonging to annihilation of the *delocalized* positrons were observed in PLT spectra. Such a picture seems to be expected, because a majority of positrons which got thermalised *inside* grains ( $\approx 20$  nm size) of the compacted YSZ nanopowders will diffuse to GB's and get trapped there. Thus it is natural to attribute the two shorter components identified in measured PLT spectra to positron trapping in two kinds of defects associated to GB's [2]: (i) the monovacancy-like defects, either the open-volume misfit defects present at GB's due to their disordered structure or the defects resembling a Zr vacancy, and (ii) the larger defects situated probably in triple points. It was also shown in Ref. [2] that the ratio of intensities observed in PLT spectra,  $I_2/I_1$ , follows the inverse proportionality to a square of mean grain size  $d$  and the proportionality constant was deduced there from a fit to the data on binary YSZ nanopowders.

One can see in table 2 that a portion of  $\approx 8\%$  of positrons form Ps in binary YSZ nanopowders. The principal oPs component ( $\tau_4 \approx 30$  ns) should be attributed annihilations of oPs localized in larger cavities of  $\approx 3$  nm size which may exist between primary particles of  $\approx 20$  nm diameter. The shorter and much weaker oPs component is likely an artifact of a nanopore size distribution.

The analysis of the CDB measurements on binary YSZ nanopowders allowed to draw several conclusions supporting the above interpretation of PLT data, see Ref. [2] for details: (i) The local chemical environment of monovacancy-like defects associated to GB's resembles that of Zr vacancies. (ii) Positrons trapped in triple points are annihilated mainly by Zr electrons. (iii) A pPs contribution is clearly visible in the region of zero

electron momenta. On the other hand, no decisive conclusion could be made about migration of Y atoms toward GB's which was reported by others [10].

Sintering experiments revealed that residual porosity (i.e., the oPs components) becomes negligible after sintering at  $T_s=1000$  °C and a significant grain growth occurs during sintering above this temperature [2].

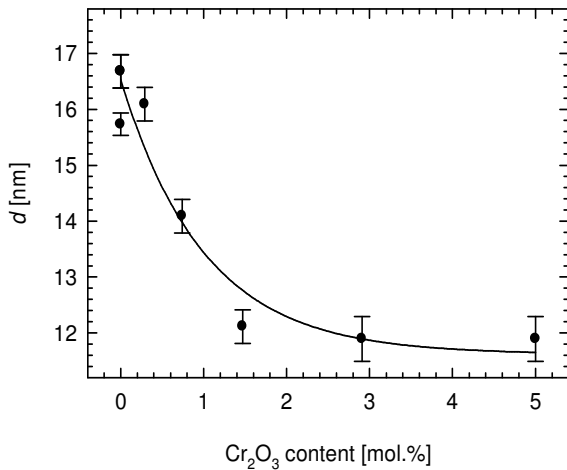


**Fig. 1.** Mean grain size  $d$  in the ternary YSZ nanopowders as a function of  $\text{Cr}_2\text{O}_3$  content.

Intensity  $I_2$  is increased with chromia content at the expense of  $I_1$ , see table 2. The correlation between the  $I_2/I_1$  ratio and mean grain size  $d$ , as disclosed for the binary YSZ's [2], was used here to estimate the mean grain size in the ternary YSZ's. The results of such procedure are presented in figure 1. Clearly, the increasing content of chromia leads to a smaller mean grain size. This is in accordance with recent findings [7] that Cr dopant inhibits particle clustering during calcinations and shifts the onset of particle coalescence toward higher temperatures.

The most distinctive feature of the PLT data for the ternary YSZ's seen in table 2 is a complete vanishing of the oPs components below the detection limit of 0.5 % even for a chromia addition as small as 0.3 mol.%. This happens obviously due to paramagnetic centres associated with Cr substituting Zr atoms in the  $\text{ZrO}_2$  lattice, rather than due to a disappearance of nanopores. Such paramagnetic centres are expected to be efficient inhibitors of Ps formation on internal surfaces of nanopores in compacted nanopowders.

The DBP ratios measured for the ternary YSZ compacted nanopowders with various chromia concentrations are plotted in figure 2. The analysis of these data was conducted in the lines similar to those used [2] in the case of the binary YSZ's. The DBP ratio measured for the pure Cr metal was plotted in fig. 2, too. It exhibits a peak centred almost at the same position as that arising from  $2p$  oxygen electrons in YSZ's

**Ternary YSZ's with chromia addition.** The two PLT components exhibiting lifetimes well below 0.5 ns were identified in the ternary YSZ samples, see table 2. By analogy with the binary YSZ's, the shorter component can be attributed to annihilations of positrons trapped in the monovacancy-like defects adjacent to GB's, while the longer of the two components arises from positrons trapped at triple points. An increase of lifetimes with increasing chromia content, pronounced especially for  $\tau_1$ , is likely an effect of a smaller Cr atomic radius compared to Y or Zr which leads to a larger open space associated with monovacancy-like defects neighbour to a Cr atom.

Intensity  $I_2$  is increased with chromia content at the expense of  $I_1$ , see table 2. The correlation between the  $I_2/I_1$  ratio and mean grain size  $d$ , as disclosed for the binary YSZ's [2], was used here to estimate the mean grain size in the ternary YSZ's. The results of such procedure are presented in figure 1. Clearly, the increasing content of chromia leads to a smaller mean grain size. This is in accordance with recent findings [7] that Cr dopant inhibits particle clustering during calcinations and shifts the onset of particle coalescence toward higher temperatures.

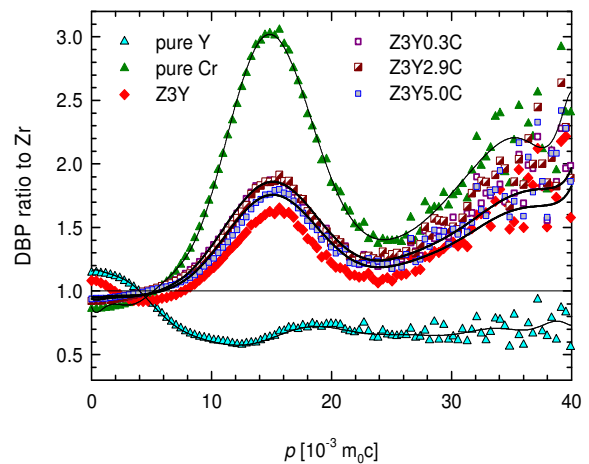


**Fig. 2.** DBP ratios vs electron momentum  $p$  for the ternary YSZ nanopowders with various content of  $\text{Cr}_2\text{O}_3$ . The thick solid lines show approximation of DBP ratio discussed in the text. The thin solid lines are plotted just to guide an eye.

[2]. Thus it is difficult to identify an effect of chromium addition to the ternary YSZ's by means of the CDB experiments. Despite of this difficulty, the observed DBP ratios for the ternary YSZ nanopowders appeared to be reasonably approximated assuming that there is a significant contribution ( $\approx 20\%$ ) of positron annihilations with the Cr inner electrons in triple points, while the chemical surroundings of the monovacancy-like defects remains unchanged (see the thick solid lines in fig. 2). It indicates that a strong Cr segregation at GB's takes place. Finally, one should note that the peak around zero electron momenta characteristic for pPs annihilations vanished in the DBP ratios measured for the ternary YSZ nanopowders.

## 5. SUMMARY

In the present paper, main results obtained recently [2] for the binary YSZ nanopowders and ceramics were reviewed. New data on the ternary YSZ nanopowders with small additions of chromia were presented. These data show that an increasing amount of the chromia additive to YSZ nanopowders leads to a smaller grain size. A segregation of Cr atoms at GB's was indicated by the CDB technique. Even the smallest amount of chromia suppresses Ps formation in YSZ's below the detection limits of the PLT and CDB techniques.

## LITERATURE REFERENCES

- [1] See, e.g., Stanford Materials Corporation web site (<http://stanfordmaterials.com/>) and links given therein.
- [2] ČÍŽEK, J., et al. Defect studies of nanocrystalline zirconia powders and sintered ceramics. *Physical Review B*, 2010, Vol. **81**, Iss. 2, Art. 024116
- [3] PROCHÁZKA, I., et al. Application of positron annihilation spectroscopy for characterization and microstructural studies of ultra fine-grained metals. From Conference Proceedings *1<sup>st</sup> Internat. Conference NANOCON 2009*. Ostrava: TANGER, 2009, pp. 45-52. ISBN 978-80-87294-13-0; also in NANOCON 2009: *1<sup>st</sup> Internat. Conference NANOCON 2009*, 20.-22.10.2009, Rožnov p. Radhoštěm, Czech Republic [CD-ROM or <http://www.nanocon.cz/en/>]. Ostrava: TANGER, 2009, paper 63. ISBN 978-80-87294-12-3
- [4] PROCHÁZKA, I., et al. Slow-positron implantation spectroscopy in nanoscience. In NANOCON 2009: *1<sup>st</sup> Internat. Conference NANOCON 2009*, 20.-22.10.2009, Rožnov p. Radhoštěm, Czech Republic [CD-ROM or <http://www.nanocon.cz/en/>]. Ostrava: TANGER, 2009, paper 70. ISBN 978-80-87294-12-3
- [5] ITO, K., NAKANISHI, H., UJIHARA, Y. Extension of the Equation for the Annihilation Lifetime of *ortho*-Positronium at a Cavity Larger than 1 nm in Radius. *Journ. Phys. Chem B*, 1999, Vol. **103**, Iss. 21, pp. 4555-4558
- [6] SLIPENYUK, A.M., et al. ESR investigation of yttria stabilized zirconia powders with nanosize particles. *Ferroelectrics*, 2004, Vol. **298**, Iss. 1, pp. 289-296
- [7] KORDUBAN, A.M., et al. X-ray photoelectron spectroscopy of nanopowders of  $ZrO_2 - Y_2O_3 - Cr_2O_3$ . *Functional Materials*, 2007, Vol. **14**, Iss. 4, pp. 454-459
- [8] BEČVÁŘ, F., et al. A high-resolution  $BaF_2$  positron-lifetime spectrometer and experience with its long-term exploitation. *Nuclear Instruments and Methods in Physics Research A*, 2000, Vol. **443**, Iss. 2-3, pp. 557-577
- [9] ČÍŽEK, J., et al. 2D-Coincidence Doppler Broadening Measurements on Neutron Irradiated VVER-Type Reactor Pressure Vessel Steels. *Materials Science Forum*, 2004, Vols. **445-446**, Iss. 1, pp. 63-65
- [10] MATSUI, K., YOSHIDA, H., IKUHARA, Y. Grain-boundary structure and microstructure development mechanism in 2-8 mol% yttria-stabilized zirconia polycrystals. *Acta Materialia*, 2008, Vol. **56**, Iss. 6, pp. 1315-1325

## Acknowledgement

***This work was financially supported by The Academy of Science of the Czech Republic in the frame of programme "Nanotechnology for Society" (project KAN30010801) and project KJB101120906, by The Ministry of Education, Youth and Sports within scientific plan MSM 0021620834 and by The National Academy of Science of Ukraine (scientific plans A 116/06 H and A 106U006933).***